

Dynamic Properties of Mixed Fullerenol/Bovine Serum Albumin Films on Water Surface

N. A. Isakov^a and B. A. Noskov^{a, *}

^a Institute of Chemistry, St. Petersburg State University, St. Petersburg, 199034 Russia

*e-mail: b.noskov@spbu.ru

Received October 19, 2022; revised November 11, 2022; accepted November 15, 2022

Abstract—The properties of a mixed fullerenol (C₆₀(OH)₂₀)/bovine serum albumin film on a water surface depend on the method of film preparation. When the components are adsorbed from a solution of their mixture, the properties of such a film are mainly determined by the protein, which is more surface-active. At the same time, the compression isotherms of such films noticeably deviate from the results obtained for the films of the pure protein. When one of the components is adsorbed on a surface that contains a film of the other component, a synergistic effect is sometimes observed. In this case, the surface pressure and the dynamic surface elasticity modulus are markedly higher than their values for solutions of individual components due to strong interactions between the components and the formation of fullerenol/protein complexes in the surface layer.

DOI: 10.1134/S1061933X22600531

INTRODUCTION

Unique properties of fullerenes attract great attention since the moment of their discovery in 1984. In particular, their ability to decrease the oxidative stress in cells, antiviral activity, and possibility to be used for targeted drug delivery are of interest from the viewpoint of medicine [1–3]. However, the use of fullerenes is substantially hindered by their low solubility in water, thereby provoking interest in their more hydrophilic derivatives. Fullerenols are most studied among water-soluble derivatives. They have a relatively low toxicity, which makes them especially applicable in medicine [4].

The biological activity of fullerenols is, to a high extent, determined by their interaction with biological macromolecules—in particular, with proteins. The formation of a protein corona around fullerenol aggregates in an aqueous system may change the tertiary structure of the protein. Fullerenol is advantageous over other carbon nanoparticles in the possibility of regulating its interaction with proteins by varying the number of hydroxyl groups in its molecule within a wide range.

The structure of a bovine serum albumin (BSA) molecule, which consists of three homologous domains, is similar to the molecular structure of human serum albumin, i.e., the main protein of blood plasma. The isoelectric point of BSA is 4.9. Therefore, at neutral pH values, the protein carries a low negative charge. As well as many other proteins, BSA exhibits a noticeable surface activity and forms adsorption layers

on a water surface. These layers have a relatively high dilatational elasticity up to 80 mN/m. Note that, when being adsorbed on a water surface, proteins may change their tertiary structure [5], thus also changing the character of their interaction with nanoparticles in a surface layer as compared with the interactions in a bulk solution.

A great deal of information is available on the interaction of proteins with fullerenes and their derivatives in aqueous bulk solutions. This information has been obtained by means of both physical [6–10], and computer experiments [6, 11–13]. The interaction between fullerene and proteins strongly depends on the sizes of fullerene aggregates in a solution. Fullerene is most efficiently bound BSA at an aggregate diameter of about 100 nm [8, 9]. Van der Waals forces and hydrogen bonding make the greatest contribution to the interaction of proteins with fullerenes. For fullerene derivatives, especially for fullerenols, the interaction with proteins is enhanced due to the π – π -interactions, which appear to be most efficient because of the small sizes of formed fullerenol aggregates [14]. It should be noted that the information on the interaction between carbon nanoparticles and proteins at interfaces is very limited in spite of its importance for explaining the interaction nanoparticles with proteins on cellular membranes.

The methods of surface dilatational rheology are highly sensitive to protein conformation in a surface layer [5, 15–17]. In this work, these methods, as well as ellipsometry, atomic force microscopy, and com-

pression isotherm measurements, have been employed to estimate the microscopic morphology, intercomponent interactions, and properties of mixed fullereneol ($C_{60}(OH)_{20}$)/BSA layers obtained by three different methods on a water surface.

EXPERIMENTAL

Initial solutions of fullereneol ($C_{60}(OH)_{20}$) (Research Centre Kurchatov Institute, Russia) and BSA (Sigma Aldrich, Germany) were prepared using a phosphate buffer solution (pH 7.00 and ionic strength $I = 0.020$ M). The buffer solution was prepared by mixing solutions of NaH_2PO_4 (Sigma Aldrich, Germany) and Na_2HPO_4 (Sigma Aldrich, Germany). Triply distilled water was used, while the second and third distillations were performed using equipment made of glass alone.

In this work, mixed fullereneol/BSA films were formed by three different methods. The first one was the joint adsorption of both components from mixed solutions. For this purpose, a mixture of initial BSA and fullereneol solutions was poured into Langmuir troughs with volumes of 100 and 330 mL, and the buffer solution was added to achieve desired fullereneol and BSA concentrations. In 10 min, the solution surface was cleaned with the help of a Pasteur pipette and a water-jet pump.

According to the second method, a fullereneol film was formed on a water surface via fullereneol adsorption from a concentrated solution for nearly 12 h. The next day, the fullereneol solution was replaced by the buffer solution, while retaining preserved the film of adsorbed fullereneol. Then, a preset volume of the initial BSA solution was introduced into the subphase with a feeder until a required BSA concentration was reached. The mixed film was formed during the subsequent penetration of BSA into the fullereneol film.

The third method for the formation of the mixed film consisted in the penetration of fullereneol into a BSA film applied onto a water surface. For this purpose, a specified volume of the initial BSA solution was applied onto the surface of the buffer solution in a Langmuir trough using an inclined glass plate and a feeder. Then, the inclined plate was withdrawn from the solution, and a concentrated fullereneol solution was introduced into the subphase. A mixed film was formed during the subsequent fullereneol adsorption.

The surface dilatational elasticity was determined by the oscillating barrier method using an ISR instrument (KSV NIMA, Finland). In this case, the oscillations of the surface area of a solution in a Langmuir trough were generated as a result of a periodic motion of two fluoroplastic barriers along the edges of the Langmuir trough. The oscillations arising in the surface pressure were measured by the Wilhelmy plate method. Complex dynamic surface dilatational elasticity $E(\omega)$ is determined by the following relation:

$$E = E_r + iE_i = |E|e^{-i\delta} = -\frac{\Delta\Pi}{\Delta A}A,$$

where ω is the angular frequency; E_r and E_i are the real and imaginary components of the dynamic surface dilatational elasticity, respectively; $|E|$ is the absolute value of the dynamic surface dilatational elasticity; δ is the phase shift between the oscillations in the surface area and the surface pressure; A is the solution surface area; and $\Delta\Pi$ and ΔA are the oscillation amplitudes of the surface pressure and surface area, respectively.

In this work, the oscillation amplitude of the surface area was 2%, which corresponded to the linear response of the system to the oscillations. The oscillation frequency of the surface area was 0.030 Hz; i.e., it lay within the operating capacity range of the used instrument (<0.1 Hz).

The sizes of the fullereneol aggregates in the aqueous solutions were determined by dynamic light scattering (DLS) with a Zetasizer ZS Nano analyzer (Malvern Instruments, United Kingdom) operating at a scattering angle of 173° .

Ellipsometry was implemented using a Multiskop instrument (Optrel GBR, Germany) operating at a laser wavelength of 632.8 nm and an angle of incidence equal to 49° , which was close to the Brewster angle. The difference between ellipsometric angles Δ and Δ_0 for solutions of a surfactant and a solvent, respectively, is proportional to the adsorption value of a dissolved component [18].

The morphologies of the layers of individual components and their mixtures were determined with an atomic force microscope (NT-MDT, Russia). For this purpose, the films were transferred from a water surface onto the surfaces of freshly cleaved mica plates by the Langmuir–Schaeffer method. Then, the plates were dried in a desiccator at 18°C for 48 h. All measurements were carried out in the tapping mode.

RESULTS AND DISCUSSION

Adsorption Films Obtained from Mixed Fullereneol/BSA Solutions

According to the DLS data, fullereneol aggregates with diameters of 4–12 nm were formed in a solution, while the average diameter was nearly 8 nm, thus being in consistence with the published results [19].

Kinetic dependences for the surface pressure (Fig. 1a) and the dynamic surface dilatational elasticity (Fig. 1b) of mixed BSA/fullereneol solutions exhibited slower variations in the surface properties as compared with the results obtained for a pure protein solution. This effect was enhanced with an increase in the fullereneol-to-BSA concentration ratio. It may be assumed that the fullereneol/BSA interaction in the bulk solution leads to the formation of relatively stable

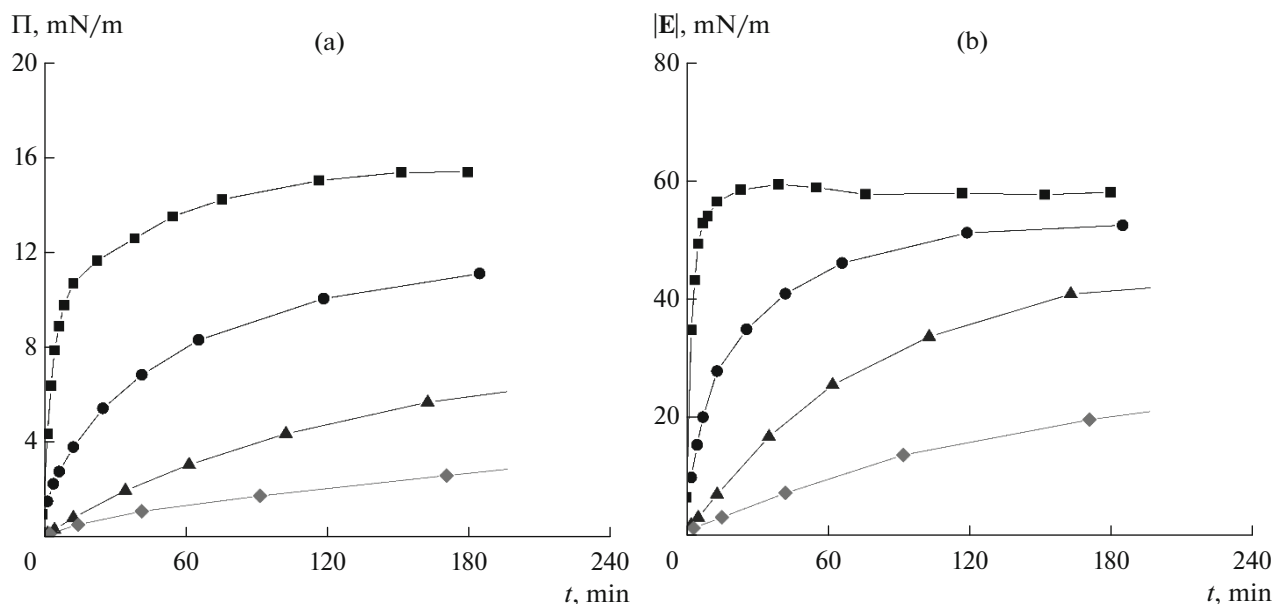


Fig. 1. Kinetic dependences of (a) surface pressures and (b) dynamic surface dilatational elasticity moduli for solutions of pure BSA (squares) and mixed $C_{60}(\text{OH})_{20}$ /BSA solutions at molar concentration ratios of 10 : 1 (circles), 100 : 1 (triangles), and 500 : 1 (rhombs). BSA concentration in the solutions is 8×10^{-7} M.

$C_{60}(\text{OH})_{20}$ /BSA complexes, thereby decreasing the concentration of free protein molecules and, hence, the rate of their diffusion to the surface. On the other hand, the rate of the adsorption of fullerene aggregates on the surface also appears to be low because of their relatively large sizes.

To obtain additional information on the basis of the kinetic curves presented in Fig. 1, the dependences of the surface elasticity modulus on the surface pressure were plotted (Fig. 2). The deviation of these dependences from the results obtained for a pure BSA solution was no larger than approximately 10%. Hence, the surface properties of the mixed solutions were mainly determined by protein adsorption.

The ellipsometry data also agree with the assumption on the predominance of BSA in the adsorption layer of the mixed $C_{60}(\text{OH})_{20}$ /BSA solution. The closeness of the kinetic dependences for the $\Delta - \Delta_0$ values of the mixed solutions and the pure BSA solution (Fig. 3) indicates close compositions of the adsorption layers of these solutions. At an initial stage of adsorption (for nearly 90 min after the formation of a new surface) the mixed solutions show a slower growth of angle Δ as compared with the results obtained for the BSA solution. This fact seems to be related to the deceleration of the diffusion to the solution surface. Relatively small differences in the kinetic dependences for the mixed solutions and the BSA solution (Fig. 3) as compared with the corresponding differences shown in Fig. 1 seem to be associated with a higher sensitivity of the surface pressure and the surface elas-

ticity modulus to the surface concentration when approaching the equilibrium state.

The above-presented data indicate only BSA adsorption from the mixed solution; however, they do not enable us to estimate adsorption of fullerene. The

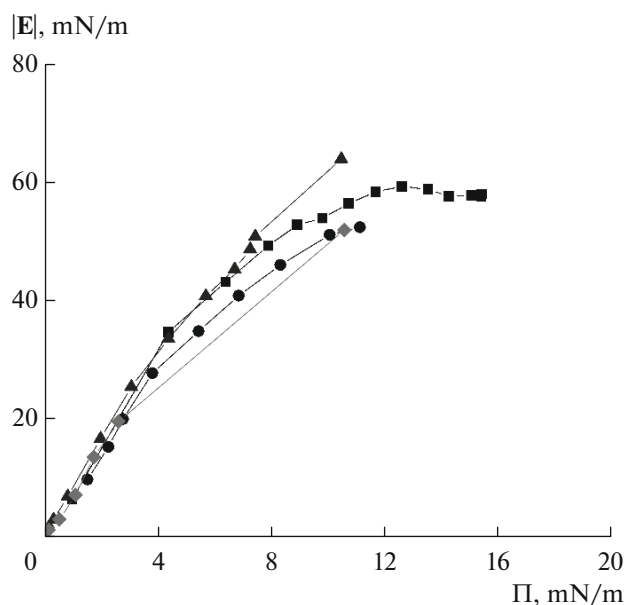


Fig. 2. Dependences of dynamic surface dilatational elasticity moduli on surface pressure for solutions of pure BSA (squares) and mixed $C_{60}(\text{OH})_{20}$ /BSA solutions at molar concentration ratios of 10 : 1 (circles), 100 : 1 (triangles), and 500 : 1 (rhombs). All data correspond to a surface age of 5 h.

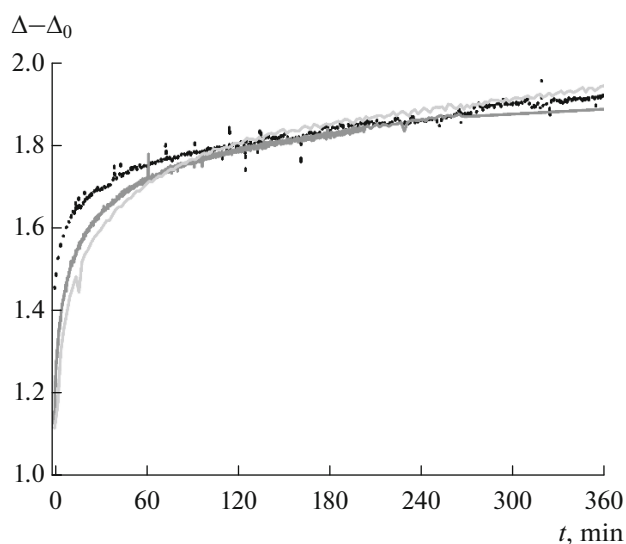


Fig. 3. Kinetic dependences of $\Delta-\Delta_0$ for solutions of pure BSA (points) and mixed $C_{60}(OH)_{20}/BSA$ solutions at molar concentration ratios of 10 : 1 (solid gray line) and 500 : 1 (solid light-gray line).

presence of fulleranol in an adsorption film manifests itself only when the film is compressed. Compression rate and initial solution surface area were $7.5 \text{ cm}^2/\text{min}$ and 517.5 cm^2 , respectively (Fig. 4). At an initial stage of compression, the surface pressure somewhat increases and remains close to the surface pressure of a pure BSA layer. Upon subsequent compression by more than 40%, deviations from the results obtained for the BSA layer become more evident. A rapid rise in the surface pressure begins earlier for mixed layers than it does for the BSA film, and the growth rate increases with the $C_{60}(OH)_{20}/BSA$ molar ratio. This seems to be associated with an enhancement of the interaction between fulleranol aggregates in the surface layer due to an increase in their local concentration. The appearance of a local maximum upon the strong compression to a surface pressure of about 50 mN/m may indicate the onset of film collapse caused by the formation of three-dimensional aggregates in an almost two-dimensional surface film. Another possible explanation may consist in a drastic acceleration of mechanical relaxation processes in the film. However, the direct measurements of the process rate after the cessation of film compression have not confirmed this hypothesis. Despite a surface pressure of 50 mN/m was reached, the pure BSA film exhibited no extreme in the surface pressure. In this case, the compression of the surface film seems to be accompanied by the continuous transfer of protein molecules from a monolayer into a sublayer with the formation of bi- and trilayers. The AFM data have shown that, after being compressed, the mixed film becomes more uniform obviously due to its densification and a gradual

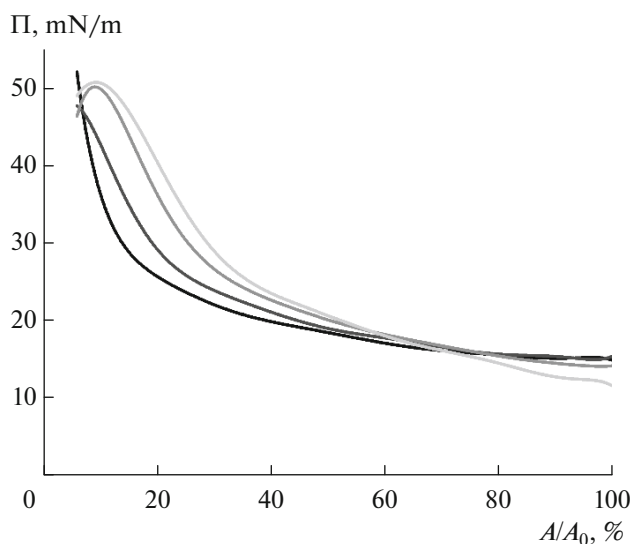


Fig. 4. Compression isotherms of adsorption films for solutions of BSA (black line) and mixed $C_{60}(OH)_{20}/BSA$ solutions at molar concentration ratios of 10 : 1 (dark-gray line), 100 : 1 (gray line), and 500 : 1 (light-gray line).

decrease in the thickness of the interaggregate gaps (Fig. 5).

Penetration of BSA into a Fulleranol Adsorption Film

BSA was adsorbed from a solution having a fulleranol film on its surface to form a mixed film with an increased surface concentration of fulleranol in accordance with the second approach. At the first stage, fulleranol was adsorbed from its solution. Then, the fulleranol solution in the cell was replaced by the phosphate buffer solution, and a concentrated BSA solution was injected into it. Subsequent adsorption of the protein caused a rapid increase in the surface pressure and the surface elasticity modulus. While approaching the equilibrium state, these parameters markedly exceeded the corresponding values for the pure BSA solution (Fig. 6). The rise in the surface elasticity is, primarily, related to a high surface concentration of fulleranol, adsorption layers of which are characterized by high values of the surface elasticity modulus [20]. The acceleration of the growth in the surface pressure and an increase in this value by 2–4 mN/m relative to the corresponding values for the pure BSA solution may indicate a change in the conformation of BSA molecules in the course of adsorption. In this case, an increase in the concentration of hydrophobic groups in the near region of the surface layer, and, hence, a rise in the surface pressure may be observed.

Repeated measurements of the surface tension and surface elasticity at the same BSA and fulleranol concentrations have shown marked discrepancies between the results, with these discrepancies exceeding the standard errors in the measurement of these values

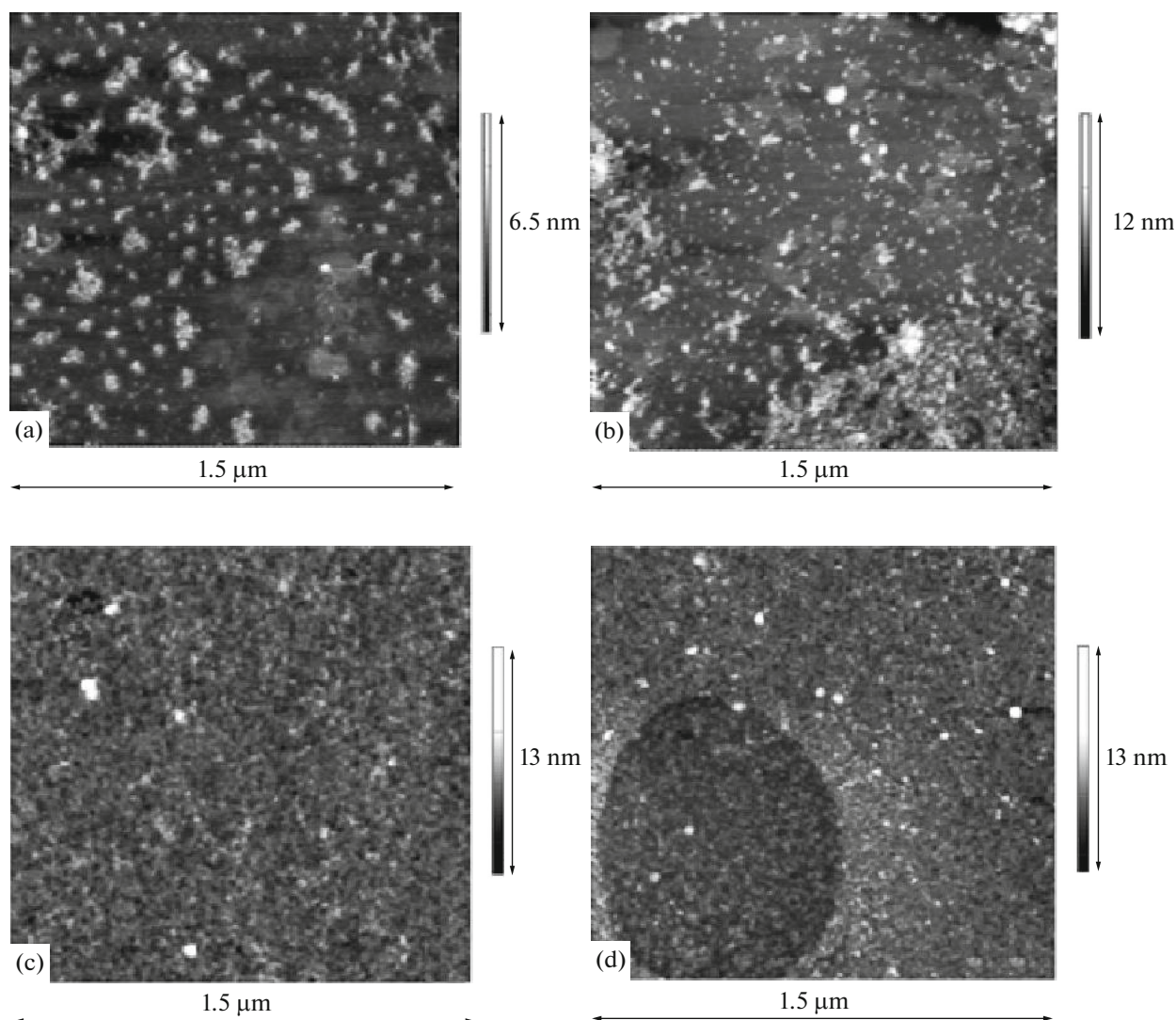


Fig. 5. AFM images obtained for $C_{60}(OH)_{20}$ /BSA adsorption films with a molar ratio of 100 : 1 20 h after the formation of a new surface (a, b) before and (c, d) after compression by 17.25 times.

(Fig. 6). This is associated with noticeable and poorly reproducible variations in the morphology of a fullerene adsorption film upon the replacement of the subphase. In this case, a relatively dense film, which mainly consists of surface fullerene aggregates with diameters of less than 50 nm, is partly dissolved. The AFM data have shown that larger “islands” unbonded to each other arise on the surface (Fig. 7). At the same time, the dynamic surface elasticity modulus decreases by 4–5 times. The properties of the subsequently formed BSA adsorption film are, to a substantial extent, predetermined by the poorly reproducible structure of an initial fullerene film and also turn out to be poorly reproducible. The nonuniformity of the mixed BSA/fullerene film is also evident from the fluctuations of the dynamic surface elasticity in the course of protein adsorption (Fig. 6).

Penetration of Fullerene into an Applied BSA Film

In the course of fullerene adsorption on an applied BSA film at different surface concentrations, the surface pressure increases from 3.5 and 8.5 to nearly 9.5 mN/m, while the surface elasticity modulus varies from 25 and 50 to 80 mN/m, thus becoming nearly 1.5-fold higher than the values characteristic of the pure BSA film (Fig. 8). The increase in the surface pressure relative to that of the fullerene solution at the same concentrations indicates the interaction between fullerene and BSA. The formation of BSA/fullerene complexes is also indicated by the great growth of the dynamic surface elasticity, with this growth being seemingly related to variations in BSA conformation upon the interaction with fullerene. At an initial stage, fullerene adsorption seemingly leads only to densification of the BSA film. Therewith, the surface properties are, as before, predetermined by protein

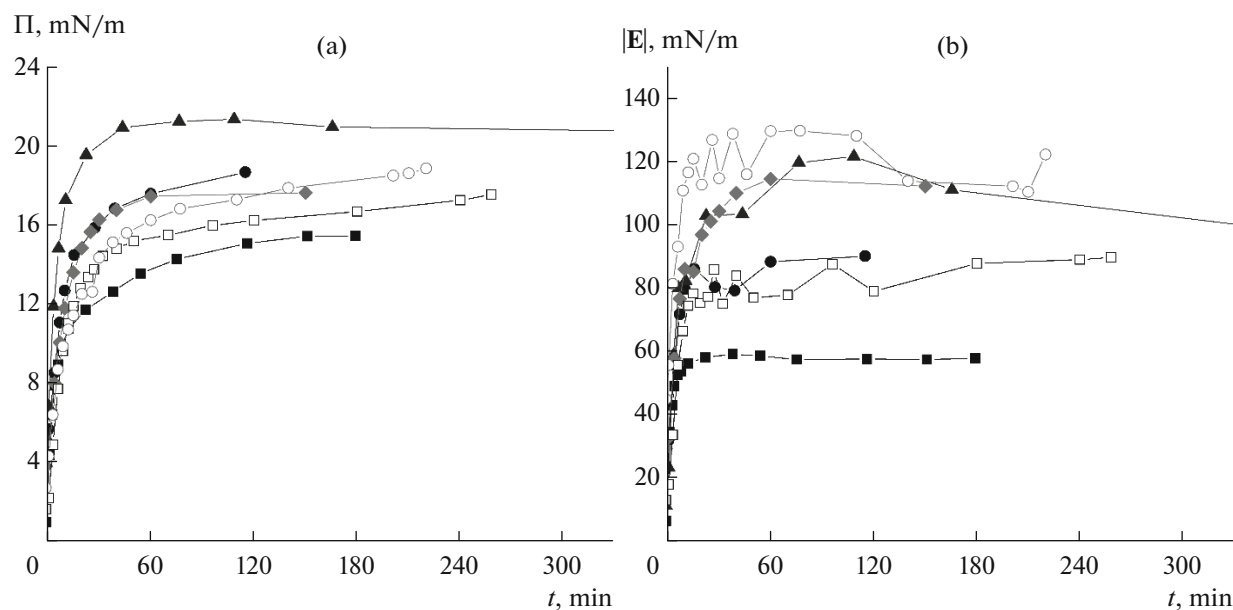


Fig. 6. Kinetic dependences of (a) surface pressures and (b) surface dilatational elasticity moduli for mixed fullerene/BSA films obtained via BSA penetration from a 7.8×10^{-7} M solution into fullerene films. Fullerene films were formed by adsorption from its solutions with concentrations of 3.9×10^{-3} (filled circles, triangles, and rhombs) and 2.3×10^{-3} (unfilled squares and circles). Filled squares refer to adsorption from a BSA solution in the absence of a fullerene film.

molecules, and the dependence of the surface elasticity on the surface pressure (Fig. 9) does not differ from the corresponding dependence for the protein solution. Then, the surface elasticity dramatically increases with relatively small changes in the surface pressure. This may indicate an increase in the local fullerene concentration primarily in the far region of the surface layer. BSA molecules, which determine the value of the surface tension, prevail in the near region of the surface layer.

Compression isotherms of mixed films resulting from the penetration of fullerene from a solution into an applied BSA film exhibit inflection points corresponding to the region of a decrease in the isotherm slope, i.e., the “quasi-plateau” region (Fig. 10). The shape of the presented curves differs from the corresponding data on the surface films obtained by the joint adsorption of fullerene and BSA, where the inflection point is absent and a local maximum is observed in the surface pressure (Fig. 4). Moreover, the films have different microscopic morphologies after compression (Figs. 5, 11). Figure 11 shows folds, which correspond to the formation of multilayer structures in the film and are not seen in the films obtained by the joint adsorption. These folds are formed at a relatively high fullerene concentration in the surface layer. The folds could be formed due to the features of the transfer of the films onto the solid substrate. However, the reproducibility of the main characteristics of the film morphology (formation of the

folds) has indicated that they are not associated with the effect of the transfer onto the solid substrate. It can be assumed that the quasi-plateau region in the isotherm corresponds to the onset of the formation of the folds, i.e., the formation of a new surface phase. Upon the further compression, the regions of the new phase begin to interact with each other, thereby increasing the curve slope.

CONCLUSIONS

The properties of a mixed fullerene/BSA film on a water surface strongly depend on the method of its formation. When a mixed film is formed via the joint adsorption, its properties are determined by the more surface-active protein. Fullerene has a marked effect only on the rate of BSA adsorption because of a reduction in the concentration of free protein molecules in the bulk solution due to the formation of BSA/fullerene complexes, which have a low mobility. In addition, the presence of fullerene in the adsorption film manifests itself as a change in the pattern of the isotherm of film compression. At high surface pressures (>45 mN/m), the isotherm becomes nonmonotonic, thus indicating the film collapse and a deterioration of its stability in the presence of fullerene.

BSA/fullerene complexes are formed in a surface layer when fullerene penetrates into an applied BSA film or BSA penetrates from a solution into a fullerene film located on a water surface. In the latter case,

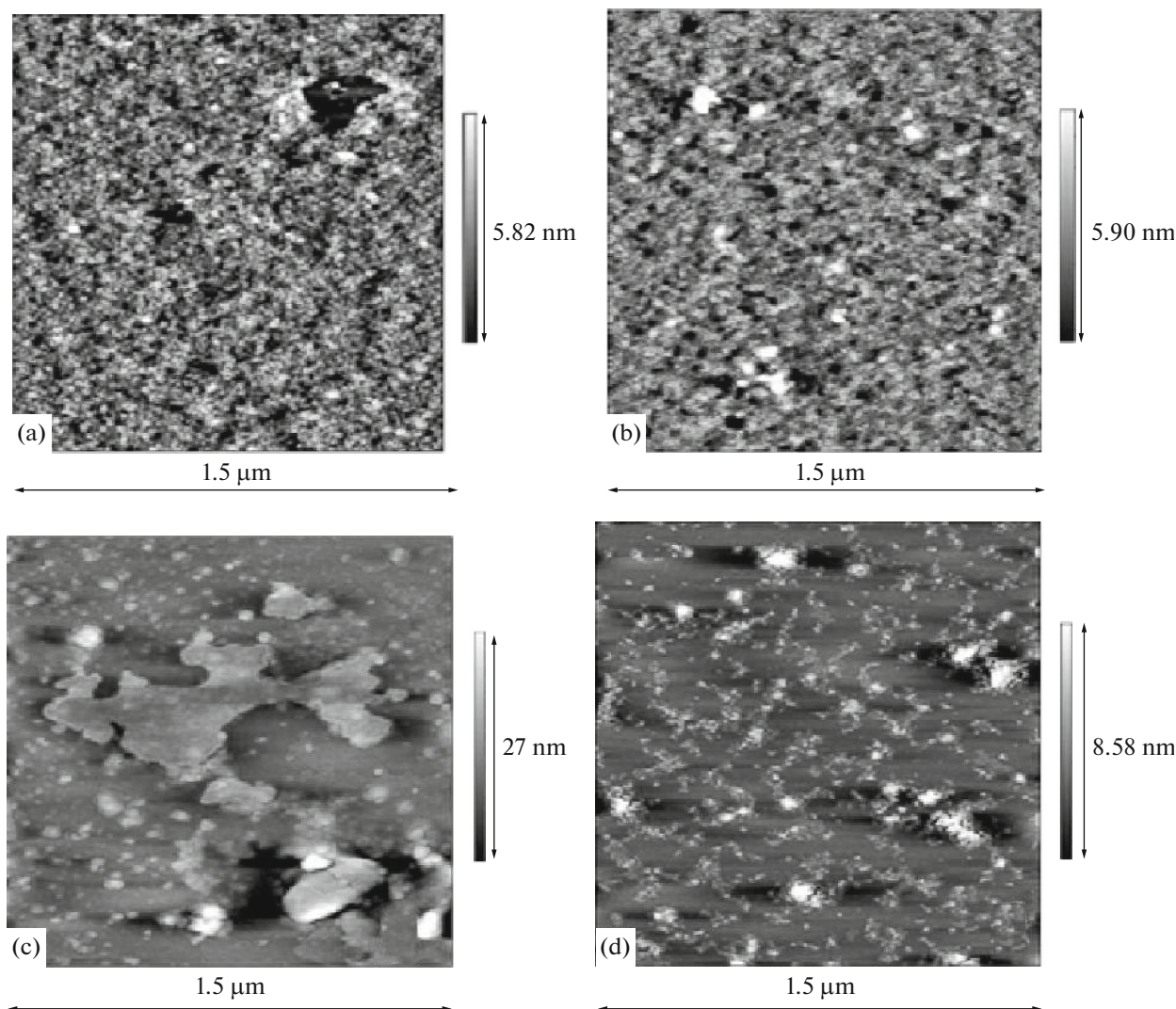


Fig. 7. AFM images obtained for mixed adsorption films of fullereneol (a, b) before and (c, d) after replacement of substrate. Initial fullereneol concentration is 4.0×10^{-3} M.

the film is formed as a result of fullereneol adsorption from its solution followed by the replacement of this solution by a buffer solution. In both cases (penetration of fullereneol into a BSA film and BSA penetration into a fullereneol film), a strong synergistic effect is observed: the surface pressure and dynamic surface elasticity markedly exceed their initial values and the values for fullereneol and BSA solutions in the first and second cases, respectively, when approaching the equilibrium, thus indicating strong intercomponent interactions in the surface layer. When a mixed film obtained via fullereneol penetration into a protein film is compressed, it becomes strongly nonuniform due to the formation of microscopic folds; however, the compression isotherms remain monotonic throughout the studied range of surface pressures (8–50 mN/m).

ACKNOWLEDGMENTS

The authors are grateful to V.P. Sedov for the synthesis of fullereneol. We are also grateful to the resource centers of the Scientific Park of St. Petersburg State University (“Methods of Analysis of Substance Composition,” “Center for Diagnostics of Functional Materials for Medicine, Pharmacology, and Nanoelectronics,” “Innovation Technologies of Composite Nanomaterials,” “Interdisciplinary Resource Center for Nanotechnologies,” and “Thermogravimetric and Calorimetric Research Methods”) for the possibility to use their equipment.

FUNDING

This work was supported by the Russian Science Foundation (project no. 21-13-00039).

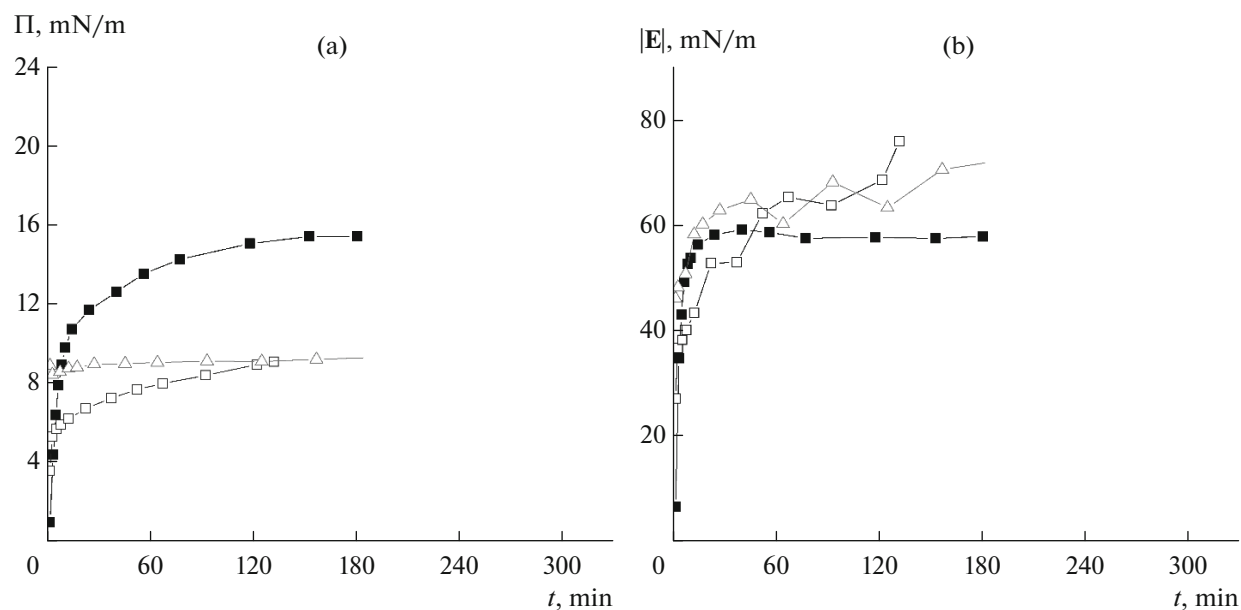


Fig. 8. Kinetic dependences of (a) surface pressures and (b) surface dilatational elasticity moduli during fullereneol penetration from a 2.3×10^{-3} M solution into an applied BSA film (unfilled triangles and unfilled squares refer to surface concentrations of 2.077×10^{-7} and 3.530×10^{-8} mol/m², respectively). Filled squares correspond to an adsorption film of BSA (7.8×10^{-7} M) free of fullereneol.

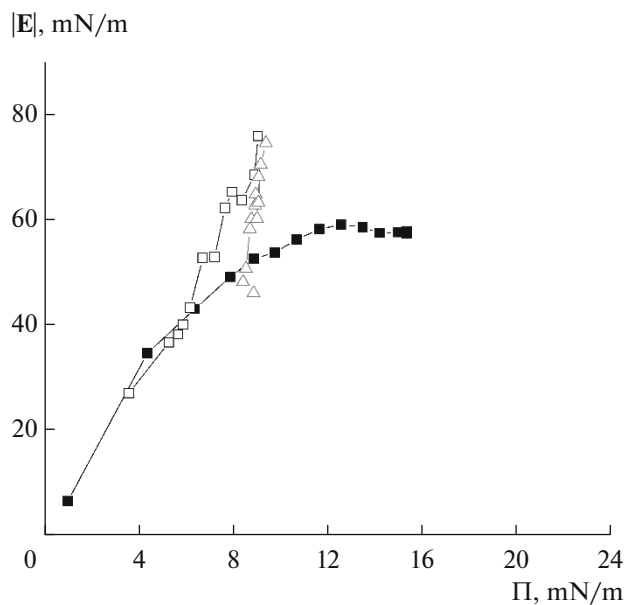


Fig. 9. Dependences of surface dilatational elasticity moduli on surface pressure for mixed fullereneol/BSA films resulting from penetration of fullereneol from a 2.3×10^{-3} M solution into applied BSA films (unfilled triangles and unfilled squares refer to surface concentrations of 2.077×10^{-7} and 3.530×10^{-8} mol/m², respectively). Filled squares correspond to adsorption film of BSA (7.8×10^{-7} M) free of fullereneol.

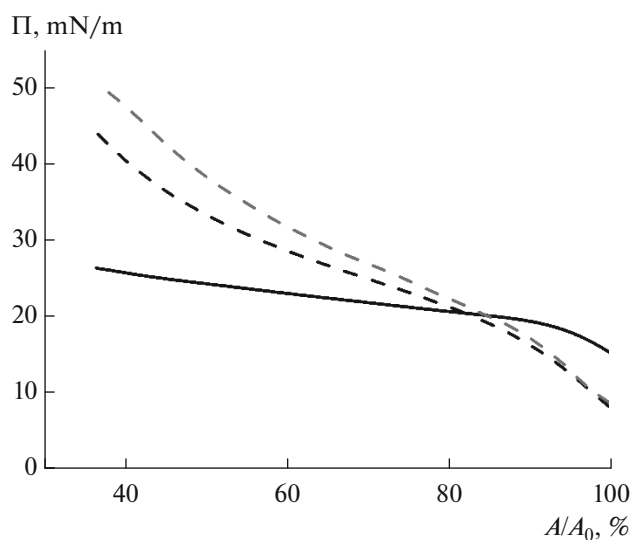


Fig. 10. Compression isotherms for mixed fullereneol/BSA films resulting from fullereneol penetration from a 2.3×10^{-3} M solution into an applied film of BSA (black dashed and light-gray dashed lines correspond to surface concentrations of 3.530×10^{-8} and 2.077×10^{-7} mol/m²). The black line corresponds to compression of BSA adsorption film (7.8×10^{-7} M) free of fullereneol.

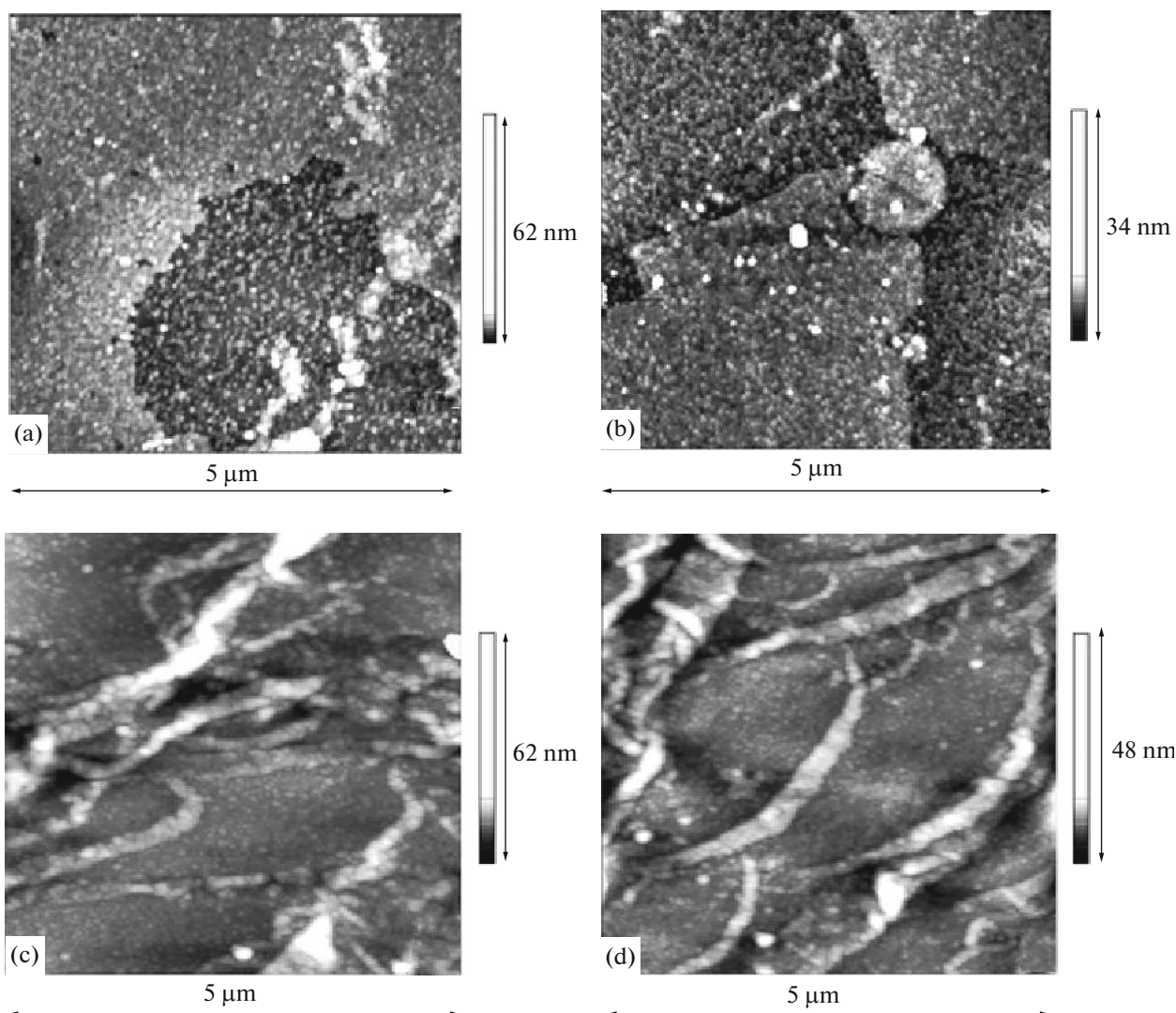


Fig. 11. AFM images of mixed fullereneol/BSA films resulting from fullereneol penetration from a 2.3×10^{-3} M solution into an applied film of BSA (3.530×10^{-8} mol/m²) (a, b) before and (c, d) after compression by 2.85 times.

CONFLICT OF INTEREST

The authors declare that they have no conflicts of interest.

REFERENCES

- Giełdoń, A., Witt, M.M., Gajewicz, A., and Puzyn, T., Rapid insight into C60 influence on biological functions of proteins, *Struct. Chem.*, 2017, vol. 28, no. 6, pp. 1775–1788.
- Castro, E., Garcia, A.H., Zavala, G., and Echevoyen, L., Fullerenes in biology and medicine, *Mater. Chem. B, R. Soc. Chem.*, 2017, vol. 5, no. 32, pp. 6523–6535.
- Kazemzadeh, H. and Mozafari, M., Fullerene-based delivery systems, *Drug Discovery Today*, 2019, vol. 24, no. 3, pp. 898–905.
- Semenov, K.N., Charykov, N.A., Postnov, V.N., et al., Fullerenols: Physicochemical properties and applications, *Prog. Solid State Chem.*, 2016, vol. 44, no. 2, pp. 59–74.
- Noskov, B.A., Protein conformational transitions at the liquid–gas interface as studied by dilational surface rheology, *Adv. Colloid Interface Sci.*, 2014, vol. 206, pp. 222–238.
- Li, S., Zhao, X., Mo, Y., et al., Human serum albumin interactions with C60 fullerene studied by spectroscopy, small-angle neutron scattering, and molecular dynamics simulations, *J. Nanopart. Res.*, 2013, vol. 15, no. 7, p. 1769.

7. Liu, S., Sui, Y., Guo, K., et al., Spectroscopic study on the interaction of pristine C60 and serum albumins in solution, *Nanoscale Res. Lett.*, 2012, vol. 7, no. 1, p. 433.
8. Fu, X., Fang, Y., Zhao, H., and Liu, S., Size-dependent binding of pristine fullerene (nC60) nanoparticles to bovine/human serum albumin, *J. Mol. Struct.*, 2018, vol. 1166, pp. 442–447.
9. Liu, S., Wang, S., and Liu, Z., Investigating the size-dependent binding of pristine nC60 to bovine serum albumin by multi-spectroscopic techniques, *Materials*, 2021, vol. 14, no. 2, p. 298.
10. Zhang, M.-F., Xu, Z.-Q., Ge, Y.-S., et al., Binding of fullerol to human serum albumin: Spectroscopic and electrochemical approach, *J. Photochem. Photobiol., B.*, 2012, vol. 108, pp. 34–43.
11. Benyamini, H., Shulman-Peleg, A., Wolfson, H.J., et al., Interaction of C 60-fullerene and carboxyfullerene with proteins: Docking and binding site alignment, *Bioconjugate Chem.*, 2006, vol. 17, no. 2, pp. 378–386.
12. Leonis, G., Avramopoulos, A., Papavasileiou, K.D., et al., A comprehensive computational study of the interaction between human serum albumin and fullerenes, *J. Phys. Chem.*, 2015, vol. 119, no. 48, pp. 14971–14985.
13. Calvaresi, M. and Zerbetto, F., Baiting Proteins with C 60, *ACS Nano*, 2010, vol. 4, no. 4, pp. 2283–2299.
14. Bai, Y., Wu, X., Ouyang, P., et al., Surface modification mediates the interaction between fullerene and lysozyme: protein structure and antibacterial activity, *Environ. Sci.: Nano*, 2021, vol. 8, no. 1, pp. 76–85.
15. Noskov, B.A., Grigoriev, D.O., Latnikova, A.V., et al., Impact of globule unfolding on dilational viscoelasticity of β -Lactoglobulin adsorption layers, *J. Phys. Chem.*, vol. 113, no. 40, pp. 13398–13404.
16. Noskov, B.A., Bykov, A.G., Gochev, G., et al., Adsorption layer formation in dispersions of protein aggregates, *Adv. Colloid Interface Sci.*, 2020, vol. 276, p. 102086.
17. Noskov, B.A., Mikhailovskaya, A.A., Lin, S.-Y., et al., Bovine serum albumin unfolding at the air/water interface as studied by dilational surface rheology, *Langmuir*, 2010, vol. 26, no. 22, pp. 17225–17231.
18. Campbell, R.A., Yanez, Arteta, M., Angus-Smyth, A., et al., Direct impact of nonequilibrium aggregates on the structure and morphology of Pdadm/SDS layers at the air/water interface, *Langmuir*, 2014, vol. 30, no. 29, pp. 8664–8674.
19. Lebedev, V.T., Kulvelis, Y.V., Voronin, A.S., et al., Mechanisms of supramolecular ordering of water-soluble derivatives of fullerenes in aqueous media, *Fullerenes, Nanotubes, Carbon Nanostruct.*, 2020, vol. 28, no. 1, pp. 30–39.
20. Akentiev, A.V., Gorniaia, S.B., Isakov, N.A., et al., Surface properties of fullereneol C60(OH)20 solutions, *J. Mol. Liq.*, 2020, vol. 306, p. 112904.

Translated by A. Kirilin